# Supported Palladium Catalysts: A Facile Preparation Method and Implications to Reductive Catalysis Technology for Water Treatment

Jinyu Gao,[†] Changxu Ren,[†] Xiangchen Huo,[‡] Rundong Ji,[†] Xiaoyu Wen,[†] Juchen Guo,[†] and Jinyong Liu*[,†]

[†]Department of Chemical and Environmental Engineering, University of California, Riverside, California 92521, United States
[‡]Department of Civil and Environmental Engineering, Colorado School of Mines, Golden, Colorado 80401, United States

**Abstract:**

Supported palladium (Pd) catalysts have been extensively studied for water purification applications. However, this technology is primarily challenged by the high cost of Pd and the lack of optimization of catalyst formulations. In this report, we demonstrate a convenient approach to prepare and optimize Pd catalysts for the reduction of toxic oxyanions (bromate, chlorate, and perchlorate). Water-dissolved $Na_2PdCl_4$ was quickly adsorbed in the suspension of activated carbon within 5 min and reduced into $Pd^0$ nanoparticles *in situ* within another 5 min under 1 atm $H_2$ at 20 °C. In terms of both material characterizations and reaction kinetics, the Pd catalysts prepared with the new method show no significant difference from those prepared by the conventional method (involving multiple-step high-temperature procedures) and from benchmark commercial Pd catalysts. With the very simple approach to control, evaluate, and optimize Pd content in the catalyst, we elucidate the relationships among the Pd content, $Pd^0$ particle size, and catalytic activity. We further showcase that the precious metals in previously reported Re−Pd/C and Mo−Pd/C catalysts can be saved for 80% without sacrificing the activity. The new and convenient catalyst preparation method will significantly enhance the cost-effectiveness of reductive catalysis technologies for water purification.

**Keywords:** Palladium catalyst, Preparation method, Metal content, Oxyanion reduction, Water purification

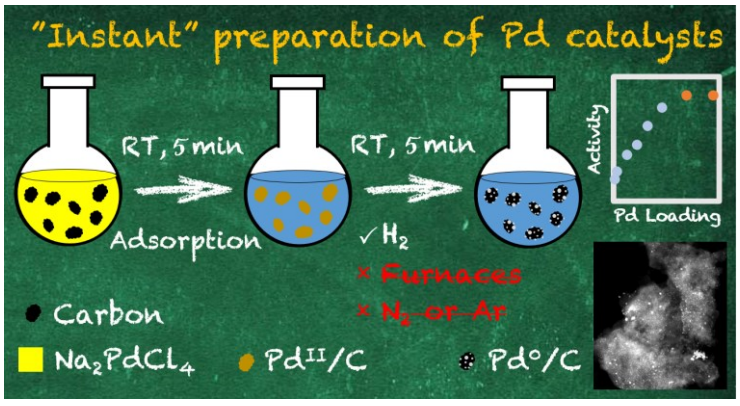

## Introduction

Supported palladium (Pd) catalysts have been extensively studied for water pollutant degradation for nearly three decades.[1-4] Toxic oxyanions, halogenated organics, and nitroso organics are labile substrates of Pd-catalyzed hydrogenation.[3] Multiple pilot systems have been studied on Pd-catalyzed degradation of chlorinated hydrocarbons[5-7] and nitrate.[2, 8] In particular, oxyanion pollutants such as bromate ($BrO_3^-$),[9-11] chlorate ($ClO_3^-$),[12-14] nitrate ($NO_3^-$),[15, 16] and perchlorate ($ClO_4^-$)[17, 18] can be only degraded through a reductive mechanism. With 1 atm $H_2$ at ambient temperatures, Pd catalysts enable complete reduction of $BrO_3^-$ and $ClO_3^-$:

$$BrO_3^- + 3\ H_2 \rightarrow Br^- + 3\ H_2O \qquad (1)$$

$$ClO_3^- + 3\ H_2 \rightarrow Cl^- + 3\ H_2O \qquad (2)$$

For highly recalcitrant substrates such as $ClO_4^-$, the incorporation of another metal, such as rhenium (Re),[19, 20] introduces a new oxygen atom transfer (OAT) mechanism that can significantly accelerate the reaction:

$$ClO_4^- + 4\ H_2 \rightarrow Cl^- + 4\ H_2O \qquad (3)$$

In addition to the widely recognized benefits of enhanced kinetics and clean byproducts, the interest in developing supported Pd catalysts is also fueled by recent discoveries of their applicability in treating waste streams, which are usually challenging to conventional wastewater treatment technologies. For example, Re–Pd/C and In–Pd/C catalysts have shown robust performance in the reduction of $ClO_4^-$ and $NO_3^-$, respectively, in waste brines from the regeneration of ion-exchange resins.[8, 21] In chloro-alkali plants, the $ClO_3^-$ byproduct in concentrated NaCl brine can be reduced back to $Cl^-$ by the currently used rhodium (Rh) catalysts or by the new Mo–Pd/C developed by our group.[22] Notably, these reactions are not significantly

inhibited (and even surprisingly accelerated)[21] by the high ionic strength in brines. In these scenarios, biological treatment may be less efficient or not feasible. Pd catalysts can be coupled with biological processes to improve the overall performance of the treatment system.[23]

However, the potential of applying hydrogenation catalysts to the broad scope of water treatment has often been challenged by the high loadings of Pd, which increases the system cost and offsets the environmental benefits of catalytic technologies. A life cycle assessment (LCA) of the previously reported Re–Pd/C for $ClO_4^-$ reduction[24] suggested that the negative environmental impacts of this technology mainly come from the use of 5 wt% Pd on the carbon support. For example, to treat 1 kg of $ClO_4^-$ by biological reactors, the total amount of $CO_2$ produced was estimated to be ~700 kg from organic electron donors, nutrients, and aeration energy. In contrast, the total amount of $CO_2$ from a 5 wt% Re – 5 wt% Pd/C catalyst was ~2000 kg, which includes 1600 kg from Pd, 250 kg from Re, and 150 kg from $H_2$ and aeration energy. If the loading of Pd can be lowered, the catalytic treatment of $ClO_4^-$ may become competitive with the biological treatment.[24] However, no effort has been made to assess the catalysts with lower Pd contents. The 5 wt% of Pd in powdered catalysts has been commonly used in a large number of studies.[3, 4] Fewer cases have used lower Pd contents such as 1 wt%,[3, 4] whereas the rationale for choosing a specific Pd content was not explicit. The effect of using lower Pd loadings for water treatment remains elusive.

Although many researchers in this field have doubts about the arbitrary choice of metal content, the preparation of a series of catalysts with various formulations for evaluation and optimization is arduous. Conventionally, supported Pd catalysts are synthesized with a combination of wet chemistry and heat treatment. For example, $Pd^{II}$ precursors are first immobilized in the porous support by various approaches (e.g., incipient wetness and alkaline

deposition).[25] Then, the powders are dried in an oven (and calcined in a muffle furnace if needed), followed by the reduction with $H_2$ gas flow at 200−500°C[25-28] with special safety measures. The whole procedure takes multiple hours, and only one catalyst formulation can be prepared each time, making it challenging to efficiently prepare and test a large variety of catalyst formulations. Therefore, it is valuable to develop a rapid, convenient, and reliable catalyst preparation method for the evaluation and optimization of catalyst formulations.

The challenges from conventional Pd catalyst preparation procedures have already triggered a broad interest in developing alternative approaches. Organic chemists have reported a "mix-and-stir" strategy to prepare Pd/C from a pre-synthesized molecular $Pd^0$ precursor, $Pd_2^0dba_3$ (*dba* = dibenzylideneacetone). In the heated organic solvent, decomposed $Pd_2^0dba_3$ complexes yielded $Pd^0$ nanoparticles on the carbon support.[29] Nanotechnology researchers synthesized $Pd^0$ nanoparticles in a solution using various chemicals and then immobilized the $Pd^0$ nanoparticles onto carbon support.[30, 31] Herein, we report on a very simple and rapid method to prepare supported Pd catalysts *in situ* with freely tunable Pd contents without heating, washing, extra chemicals, or special equipment. We used material characterizations, reaction kinetics, and case studies to show that the new method allows for rapid and extensive screening and optimization of supported Pd catalysts to advance catalyst development for water treatment, where cost-effectiveness is a primary focus.

## Materials and Methods

**Chemicals and materials**. $KBrO_3$, $NaClO_3$, $NaClO_4$, $Na_2PdCl_4$, $KReO_4$, and $Na_2MoO_4$ (>98% purity for each) were used as received from Sigma−Aldrich. Detailed information of commercial Pd catalysts and the support materials (activated carbon, aluminum oxide, and silica

gel) for Pd catalyst preparation are summarized in **Table S1** of the **Supporting Information** (**SI**). All aqueous solutions were prepared with Milli-Q water (resistivity >18.2 MΩ cm). The solution pH was adjusted by 2 N $H_2SO_4$ standard solution (Alfa Aesar) for pH 3.0 and by the mixed solution of 5 mM $Na_2HPO_4$ and 5 mM $NaH_2PO_4$ (Fisher Chemical) for pH 7.2.

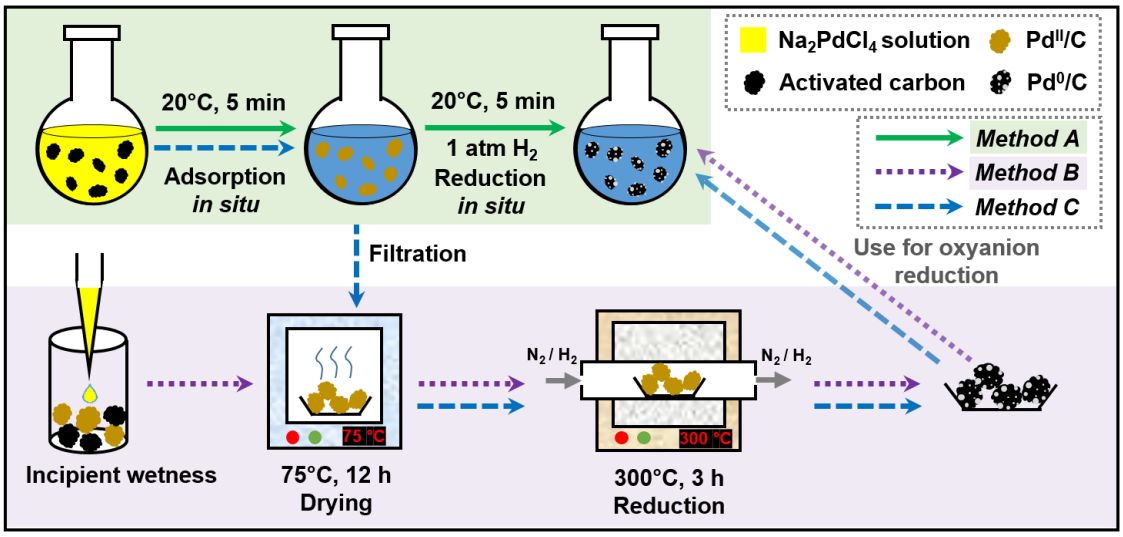


**Figure 1.** Preparation of Pd/C catalysts with three different approaches.

**Pd/C catalyst preparation.** This work developed the *all-in-situ Method A* to prepare supported Pd catalysts (**Figure 1**). A 50-mL flask was sequentially loaded with a magnetic stir bar, the desired amount of carbon, 50 mL of DI water, and the desired amount of $Na_2PdCl_4$ (via stock solution). The flask was capped with a rubber stopper and sonicated for 1 min to disperse the carbon particles. Two 16-gauge stainless steel needles were introduced through the stopper. One needle was connected to the $H_2$ gas supply, and the other one served as both the gas outlet and sampling port. The whole operation was conducted at room temperature (20°C). The suspension was stirred at 350 rpm for 5 min to allow the adsorption of the $Pd^{II}$ precursor. Afterward, the suspension was sparged with $H_2$ (2−3 mL $min^{-1}$) for another 5 min to reduce the adsorbed $Pd^{II}$ into $Pd^0$. The concentration of Pd in water was analyzed by inductively coupled plasma−optical

emission spectrometry (ICP−OES, PerkinElmer Optima 8300). The preparation of $Pd/Al_2O_3$ and $Pd/SiO_2$ followed the same procedure.

To validate the new *Method A*, we also prepared Pd/C using the same carbon material with conventional *Method B*, which uses incipient wetness for the impregnation of $Pd^{II}$ into carbon support and then a heated $H_2$ flow to reduce $Pd^{II}$ into $Pd^0$. In a 7-ml scintillation vial, 100 mg of dry carbon powder was loaded as a 0.5-cm-thick cake. $Na_2PdCl_4$ (13.8 mg, containing 5 mg Pd) was dissolved in 100 μL of DI water and slowly added via a pipette tip to wet the entire carbon cake without accumulating liquid at the vial bottom. The resulting wet paste was loaded on a small sample boat made of aluminum foil, dried in a 75°C oven for 12 h, and then transferred into a tube furnace. The tube furnace was first flushed with $N_2$ for 30 min at room temperature to avoid mixing $H_2$ and air. After switching to $Ar/H_2$ (v/v = 95/5), the furnace was heated at 300°C for 3 h. The furnace was then cooled down for 2 h and flushed with $N_2$ for another 30 min before taking out the sample boat.

To directly compare the effect of *in situ* reduction at 20°C and heated reduction at 300°C, we also used *Method C*, where the adsorption of $Pd^{II}$ occurred in water suspension (the same as *Method A*) and the $H_2$ reduction occurred in the tube furnace (the same as *Method B*).

**Oxyanion reduction.** After catalyst preparation, pH buffers and oxyanions ($BrO_3^-$, $ClO_3^-$, and $ClO_4^-$) were added to the catalyst suspension to initiate the reaction under the sparging of 1 atm $H_2$ (2−3 mL $min^{-1}$) at 20°C. For $ClO_4^-$ reduction, the $KReO_4$ precursor was added to the Pd/C suspension (pH 3.0) under $H_2$ sparging for 8 h to prepare the Re−Pd/C catalyst.[21] For $ClO_3^-$ reduction by Mo−Pd/C, the $Na_2MoO_4$ precursor was added to the Pd/C suspension (pH 3.0) under $H_2$ sparging for 15 min.[22] Reactions using all other Pd catalysts followed the same procedure. Aliquots of water samples were collected with a 3-mL syringe and immediately filtered through a

0.22-μm cellulose acetate membrane. Concentrations of anions were determined by ion chromatography (Dionex ICS−5000) equipped with a conductivity detector and a 25 μL sample injection loop. For $BrO_3^-$ and $ClO_3^-$, an IonPac AS19 column and 20 mM KOH eluent were used. For $ClO_4^-$, an IonPac AS16 column and 65 mM KOH eluent were used. The column temperature was 30℃, and the eluent flow rate was 1 mL $min^{-1}$.

**Catalyst characterization.** The prepared Pd/C powder was washed with DI water and collected by filtration under vacuum. The filter paper with the catalyst cake was placed in a fume hood and dried by the airflow at room temperature. The Pd content was measured by ICP−OES after digestion with $HCl/HNO_3$. The oxidation state of Pd was determined by X-ray photoelectron spectroscopy (XPS, Kratos AXIS Supra). X-ray diffraction (XRD) of Pd/C powders was conducted with a Panalytical Empyrean instrument (45 kV/40 mA) equipped with a Cu-Kα source. The surface area of Pd was determined by chemisorption using a Micromeritics ASAP 2020 analyzer with the surface Pd:CO stoichiometry of 2.[32] All Pd/C powders were resuspended and sonicated in distilled water to further reduce the size for characterization by a scanning transmission electron microscope (STEM, FEI Titan Themis 300) equipped with an energy dispersive X-ray spectrometer (EDS) system at 300 kV accelerating voltage. STEM images were acquired with a high-angle annular dark-field (HAADF) detector. The statistical analysis of Pd particle size was performed using the Nano Measurer software package.

## Results and Discussion

**Catalyst preparation and characterization.** The reduction of dissolved $Pd^{II}$ into $Pd^0$ by 1 atm $H_2$ at room temperature has been documented for at least 35 years.[33, 34] We verified this phenomenon with a very simple experiment using only an aqueous solution of $Na_2PdCl_4$ and 1 atm $H_2$ in the headspace. Within 35 min, the yellow color of the $Pd^{II}$ solution completely faded, and

gray $Pd^0$ solids precipitated out (**Figure S1a**). Beneath the solution surface, the reduction occurred with the diffusion of $H_2$ (**Figure S1b**). We hypothesized that if $Pd^{II}$ is dispersed in a porous material, the reduction by 1 atm $H_2$ at ambient temperature will yield dispersed $Pd^0$ nanoparticles. Hence, we expected that this approach could avoid multiple-step procedures in the conventional preparation method.

We chose $Na_2PdCl_4$ as the $Pd^{II}$ precursor because it has good solubility in water and only leaves $Na^+$ and $Cl^-$ after the reduction. A comprehensive discussion of various $Pd^{II}$ precursors and conventional catalyst preparation methods can be found in the literature.[25, 32] ICP−OES analysis of dissolved Pd found that, in the absence of $H_2$, 98% of the added Pd (5.0 mg $L^{-1}$) was adsorbed into activated carbon (100 mg $L^{-1}$ suspension) within 5 min. The dissolution of $Na_2PdCl_4$ generated $Pd^{II}$ colloids (confirmed by the Tyndall effect, **Figure S2**) and lowered the pH of DI water (**Table 1**), indicating the following process that combines ligand exchange, hydrolysis, and polymerization of $Pd^{II}$:[25, 35-37]

$$m\,[PdCl_4]^{2-} + mn\,H_2O \rightarrow [Pd(OH)_x(OH_2)_{n-x}Cl_{4-n}]_m^{m(2-n+x)-} + mx\,H^+ + mn\,Cl^- \qquad (4)$$

where $n$ and $x$ can be any value between 0 and 4 ($n \geq x$) depending on solution conditions. The following $H_2$ sparging further lowered the dissolved Pd from 0.11 mg $L^{-1}$ to below the detection limit (0.01 mg $L^{-1}$) within 5 min. This result indicates >99.8% removal of Pd from the aqueous phase. The exposure to $H_2$ for only 3 min provided the full activity for catalytic reduction of $BrO_3^-$ (**Figure S3**), suggesting a rapid reduction of the adsorbed $Pd^{II}$ precursor into active $Pd^0$ particles. Elemental analysis of the resulting Pd/C found 4.52 wt% of Pd, which is close to the theoretical value of 4.76% (i.e., 5 mg of Pd was added to 100 mg of carbon). Upon $H_2$ sparging, the pH of the aqueous phase was further lowered (**Table 1**), indicating the reduction of adsorbed $Pd^{II}$ species:

$$[Pd(OH)_x(OH_2)_{n-x}Cl_{4-n}]_m^{m(2-n+x)-} + m\,H_2 \rightarrow Pd^0{}_m + m(2-x)\,H^+ + m(4-n)\,Cl^- + mn\,H_2O \qquad (5)$$

The overall reaction combining Eqs 4 and 5 is

$$m\,[PdCl_4]^{2-} + m\,H_2 \rightarrow Pd^0{}_m + 2m\,H^+ + 4m\,Cl^- \qquad (6)$$

**Table 1. The Changes of Solution pH after Sequential Steps for Pd/C Preparation**[a]

| Pd content (wt %) | DI Water | after addition of $Na_2PdCl_4$ | after addition of carbon | after $H_2$ sparging |
|---|---|---|---|---|
| 0.5 | 6.53 | 5.50 | 5.95 | 4.86 |
| 5 | 6.62 | 4.93 | 5.00 | 3.96 |

[a]The loading of carbon was 0.1 g $L^{-1}$, and the added Pd concentrations for preparing 0.5 and 5 wt% Pd/C were 0.5 and 5.0 mg $L^{-1}$, respectively.

The exposure of $Na_2PdCl_4$ solid to 1 atm $H_2$ quickly changed the color from brown to metallic (**Figure S4**), suggesting that an aqueous environment is not critical for the rapid reduction of $Pd^{II}$ into $Pd^0$. We added ethylenediaminetetraacetic acid and citric acid to the solution of $Na_2PdCl_4$ to simulate the effect of typical functional groups on carbon (e.g., carboxylate, hydroxyl, and amino). Interestingly, both additives slowed down the reduction of $Pd^{II}$ in bulk solution (**Figure S5**). Thus, the potential interaction between adsorbed $Pd^{II}$ and surface functional groups might impede Pd reduction. Nevertheless, characterization data below show that highly dispersed $Pd^{II}$ in the carbon support was rapidly and fully reduced to $Pd^0$ nanoparticles.

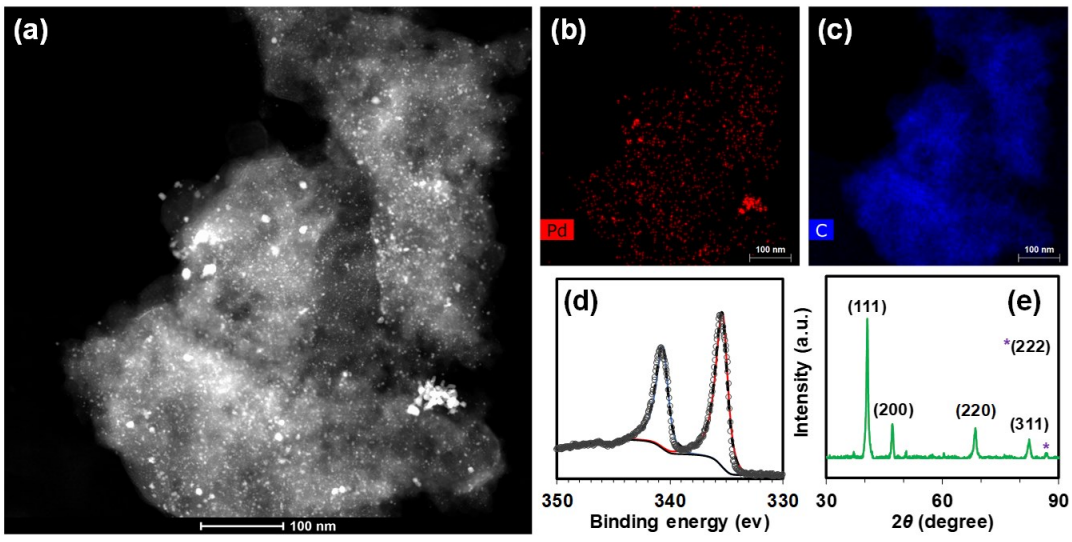


**Figure 2.** (a) HAADF-STEM imaging, EDS mapping of (b) Pd and (c) C, (d) Pd 3d XPS spectrum, and (e) powder XRD spectrum of the 5 wt% Pd/C catalyst prepared by *Method A*.

194 The STEM characterization observed a good dispersion of Pd in the carbon support (**Figure**
195 **2a**). EDS elemental mapping confirmed the bright spots in the HAADF-STEM image as Pd
196 nanoparticles (**Figure 2b**). Macropores of the activated carbon can be seen in the elemental
197 mapping of C (**Figure 2c**). XPS characterization observed only one set of Pd 3d spin-orbit coupling
198 doublets (**Figure 2d**), with the $3d_{5/2}$ binding energy at 335.5 eV. This value is characteristic of
199 $Pd^0$.[22] Notably, the airflow drying without heating did not oxidize the surface of $Pd^0$ nanoparticles
200 to $Pd^{II}O$. Five peaks corresponding to $Pd^0$ crystals were identified in the XRD spectrum (**Figure**
201 **2e**). These peaks showed little difference from those of the commercial Pd/C catalyst (**Figure S6**)
202 and other carbon-supported Pd catalysts[27] in terms of the diffraction angles and relative intensities.

203 In the STEM images, the majority of adsorbed $Pd^{II}$ was converted into fine particles of $Pd^0$,
204 whereas some relatively large $Pd^0$ particles can be seen on the edge of the carbon. More STEM
205 images are available in **Figure S7**. We postulate that the formation of those large $Pd^0$ particles is
206 attributed to the deposition of the residual dissolved Pd (i.e., 0.11 mg $L^{-1}$ in the bulk solution)
207 upon $H_2$ sparging. It is also possible that $Pd^0$ particles initially formed in the solution can also be
208 captured by the carbon support.[31] We note that $Pd^0$ catalysts from the reduction of $Pd^{II}$ within solid
209 supports usually contain $Pd^0$ particles in a wide size range.[25, 27, 29, 38, 39] A narrow size distribution
210 of $Pd^0$ particles is primarily achieved via solution-phase synthesis using special chemicals.[31, 40]

211 **Validation of catalyst structure and performance**. We compared the Pd/C catalysts
212 prepared by *Methods A*, *B*, and *C* (**Figure 1**) and a commercial Pd/C, which has been used in early
213 studies as a benchmark catalyst.[20, 22, 27, 41, 42] STEM characterization of all four Pd/C observed
214 similar distribution and size of $Pd^0$ particles (**Figure S7**−**S10**). For catalytic reduction of $BrO_3^-$,
215 the Pd/C prepared by *Method A* showed the highest activity (**Figure 3a**). At pH 7.2, the use of 0.1
216 g $L^{-1}$ Pd/C achieved 95% reduction of 1 mM $BrO_3^-$ within 1 h. The commercial Pd/C was also

more active than those prepared by *Method B* and *C*, which involved heated $H_2$ treatment. The effect of temperature and time for $Pd^0$ formation (20°C for 5 min in *Method A* versus 300°C for 3 h in *Method B*) and the effect of $Pd^{II}$ immobilization (incipient wetness in *Method B* versus aqueous adsorption in *Method C*) remain elusive and go beyond the scope of this study. However, the results confirm that the *all-in-situ Method A* provided a Pd/C with satisfactory activity. In comparison to the labile $BrO_3^-$, the reduction of $ClO_3^-$ required acidic pH 3.0 and 0.5 g $L^{-1}$ of Pd/C.[41] The *all-in-situ* prepared and commercial Pd/C catalysts showed similar activities (i.e., only 28% difference in rate constants); both reduced >95% of 1 mM $ClO_3^-$ within 8 h (**Figure 3b**).

The reduction of highly recalcitrant $ClO_4^-$ required the use of a bimetallic Re–Pd/C catalyst at a high loading of 2.0 g $L^{-1}$ at pH 3.0. The $Re^{VII}O_4^-$ precursor is reduced by $H_2$+Pd/C into surface-immobilized $Re^{V}O_x$ clusters and $Re^{I}$ species.[43] The $Re^{V}$ site abstracts one oxygen off the $Re^{V}$-bound $ClO_4^-$ and other $x<4$ $ClO_x^-$ products:

$$ClO_x^- + Re^{V}O_y \rightarrow ClO_{x-1}^- + Re^{VII}O_{y+1} \qquad (7)$$

The $Re^{V}$-$Re^{VII}$ redox cycle is maintained by Pd-catalyzed hydrogenation:

$$Re^{VII}O_{y+1} + H_2 \rightarrow Re^{V}O_y + H_2O \qquad (8)$$

Interestingly, the Re–Pd/C catalyst from the *all-in-situ* prepared Pd/C showed a 6-fold higher $ClO_4^-$ reduction activity than that from the commercial Pd/C (**Figure 3c**). We note that the rate-limiting step of $ClO_4^-$ reduction is the reaction between $ClO_4^-$ and $Re^{V}$, and the reactivity of $Re^{V}$ is influenced by its coordination environment,[20, 21, 44] including the functional groups on carbon materials. Hence, a comparison between the two Pd/C in the perspective of reducing $Re^{VII}$ to $Re^{V}$ is not meaningful. However, the much higher activity from the *all-in-situ* prepared Pd/C demonstrates the importance of testing new supports to improve the catalyst performance. Such

an effort can be significantly accelerated by the convenient *all-in-situ* method for catalyst preparation.

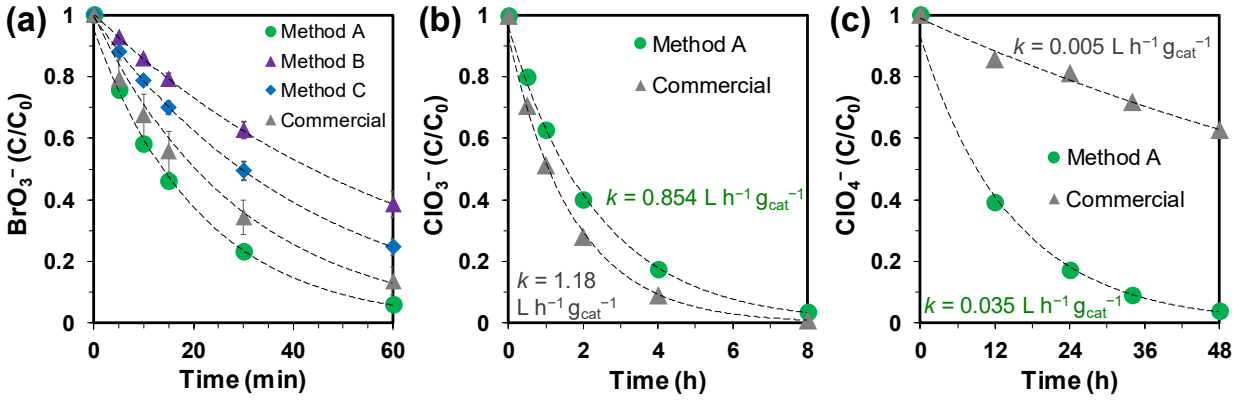


**Figure 3.** The reduction of (a) 1 mM $BrO_3^-$ by 0.1 g $L^{-1}$ of 5 wt% Pd/C at pH 7.2, (b) 1 mM $ClO_3^-$ by 0.5 g $L^{-1}$ of 5 wt% Pd/C at pH 3.0, and (c) 1 mM $ClO_4^-$ by 2.0 g $L^{-1}$ of 5 wt% Re – 5 wt% Pd/C at pH 3.0. All reactions used 1 atm $H_2$ at 20°C. Catalysts prepared by *Methods A–C* used the same carbon support. Dotted lines indicate the first-order model fit.

We further confirmed the robustness of Pd/C prepared by the *all-in-situ Method A*. First, the recycled (i.e., centrifuged, collected, and redispersed) Pd/C showed an almost identical performance to the freshly prepared Pd/C in water suspension (**Figure S11**). The spikes of 1 mM $BrO_3^-$ into the Pd/C suspension for five times resulted in a gradual but limited loss of activity (**Figure S12a**). However, the almost identical kinetics for 1 mM $BrO_3^-$ reduction in the presence of 4 mM NaBr by the fresh Pd/C (**Figure S12b**) shows that the activity decrease during catalyst reuse was merely caused by the accumulation of $Br^-$ in water. Furthermore, the *all-in-situ* prepared and commercial Pd/C were both resistant to 2 M NaCl and 1 M $Na_2SO_4$ for $BrO_3^-$ reduction at pH 7.2 (**Figure S13**).

Besides the carbon support, we also applied the *all-in-situ Method A* to load 5 wt% of $Pd^0$ on $Al_2O_3$ and $SiO_2$. In general, Pd/$Al_2O_3$ and Pd/$SiO_2$ were less active than Pd/C in $BrO_3^-$ reduction (**Figure S14**). The *all-in-situ* prepared and commercial Pd/$Al_2O_3$ and Pd/$SiO_2$ showed similar activities (**Figure S15**). Although the diverse structure of support materials can impact the catalyst

activity (out of the scope of this work), the results clearly show that the *all-in-situ* catalyst preparation using 1 atm $H_2$ at 20°C can be applied to multiple support materials.

**Effect of Pd content on catalytic activity.** We utilized this new catalyst preparation method to systematically optimize the formulation of Pd/C. Although it seems common sense that the variation of Pd contents will alter the catalytic activity, a quantitative relationship has not yet been determined for oxyanion reduction. We prepared eight Pd/C with a variety of Pd contents (0.5, 1, 3, 5, 7, 10, 15, and 20 wt%) by simply controlling the dose of $Na_2PdCl_4$ added in the water suspension. At the same loading of the carbon support (0.1 g $L^{-1}$), the rate of $BrO_3^-$ reduction increased when the Pd content increased from 0.5 wt% to 10 wt%, and reached a plateau beyond 10 wt% (**Figure 4a**). However, in the Pd content range of 0.5−10 wt%, the increase of Pd for 100% only increased the rate constant for 60%. Chemisorption data suggest that the increased Pd content decreased the surface area normalized by the mass of Pd (**Figure 4b**). STEM characterization confirms that the average size of $Pd^0$ particles in 0.5 wt% Pd/C is half of that in 5 wt% Pd/C (**Figure 5**, and **Figure S16** versus **S7**). The majority of $Pd^0$ particles in 0.5 wt% Pd/C are smaller than 2 nm. We note that the $Pd^0$ surface coverage by the residual $Cl^-$ (from $Na_2PdCl_4$) led to a significantly reduced CO chemisorption (**Table S2**).[25, 30] Therefore, the calculated average sizes of $Pd^0$ particles are much larger than the STEM measurements.

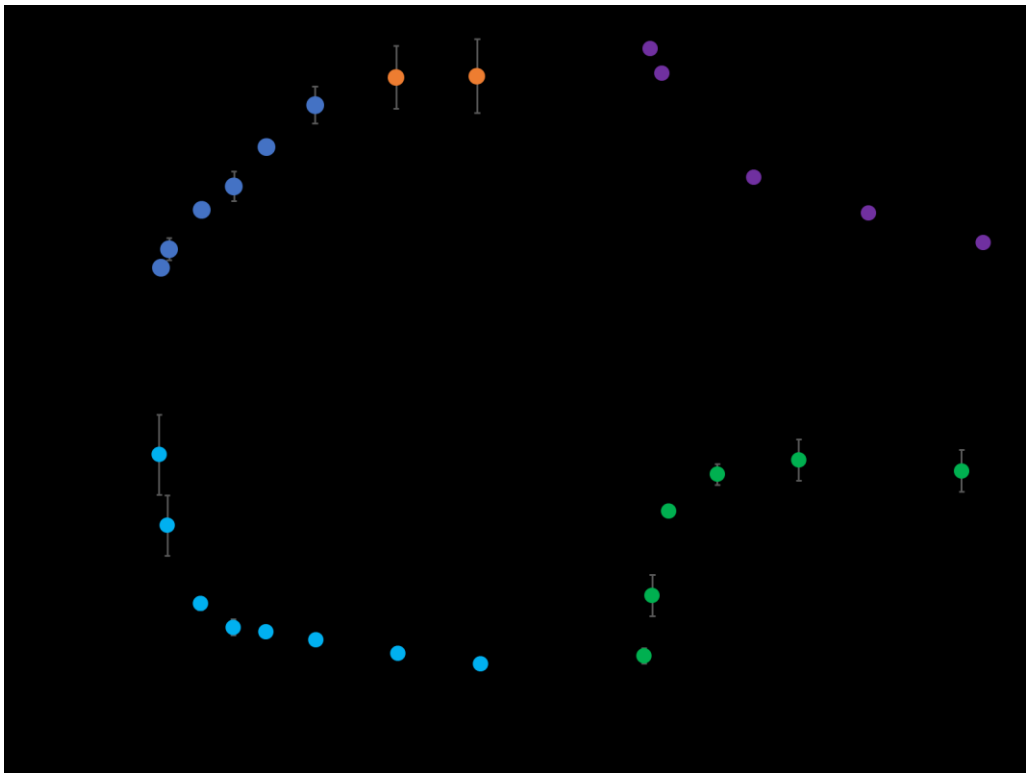

**Figure 4.** Relationships for the *all-in-situ* prepared Pd/C catalysts with various Pd contents. The rate constants ($k$) in panels **a** and **c** represent the reduction of 1 mM $BrO_3^-$ with 0.1 g $L^{-1}$ Pd/C (pH 7.2, 1 atm $H_2$, and 20°C). For panel **d**, 5 mg $L^{-1}$ Pd was dispersed into different loadings of carbon support, thus yielding various weight percentages for Pd.

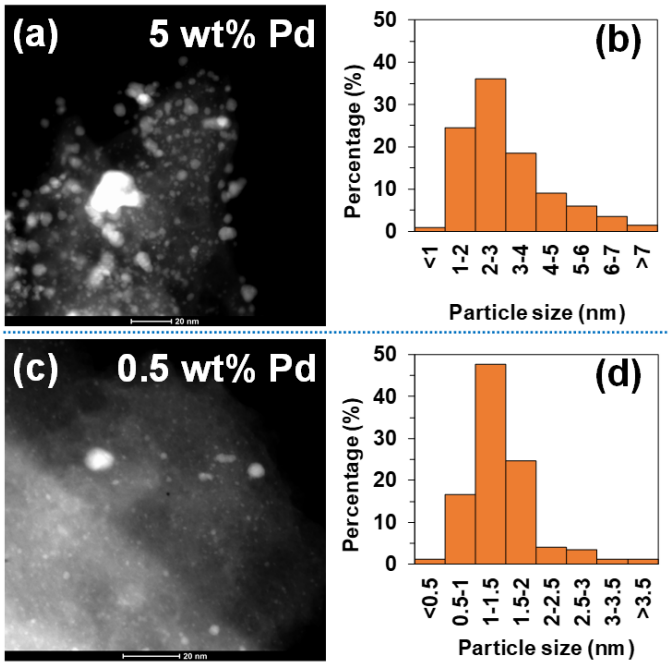


**Figure 5.** HAADF-STEM imaging and $Pd^0$ particle size distribution histograms of *all-in-situ* prepared 5wt% Pd/C (panels a and b) and 0.5 wt% Pd/C (panels c and d).

We normalized the rate constants of $BrO_3^-$ reduction (in $min^{-1}$) by the total loading of Pd in the water suspension (in $g_{Pd}\ L^{-1}$). **Figure 4c** shows that a low Pd content of 0.5 wt% is 2.5 fold more cost-effective than 5 wt%. We consolidated this finding by using different loadings of carbon (0.05–2 g $L^{-1}$) to accommodate the same amount of Pd (5 mg $L^{-1}$). **Figure 4d** shows that 0.5 wt% Pd/C (i.e., dispersing 5 mg $L^{-1}$ Pd into 1.0 g $L^{-1}$ of carbon) provided the highest reaction rate. Further increasing the carbon loading to 2.0 g $L^{-1}$ (i.e., 0.025 wt% Pd/C) did not enhance the catalytic activity further but wasted the carbon support. These quantitative observations from rapid testing of multiple Pd/C formulations are attributed to the convenient *all-in-situ* preparation method.

**Case study 1: Optimization of the Re–Pd/C catalyst.** After identifying that a low Pd content (e.g., 0.5 wt%) on the carbon support can maximize the cost-effectiveness of $Pd^0$, we optimized the Re–Pd/C catalyst, where both Pd and Re were 5 wt% for $ClO_4^-$ reduction in the earlier LCA study.[21, 24] When we lowered both Pd and Re contents by 90% (i.e., to 0.5 wt% for each metal), the rate of $ClO_4^-$ reduction was only reduced for 46% (**Table 2**, entry 6 versus 2). Because the apparent rate constants are in proportion to the catalyst loadings,[19, 20, 45] a doubled loading (4 g $L^{-1}$) of the new 0.5 wt% Re – 0.5 wt% Pd/C catalyst achieved the same kinetics as 2 g $L^{-1}$ of 5 wt% Re – 5 wt% Pd/C (**Figure 6a)**. Therefore, in comparison to the original configuration, a doubled amount of carbon support and a 20% amount of both Pd and Re afforded the same performance of $ClO_4^-$ reduction. If the same LCA metrics are used, the calculated $CO_2$ can be lowered from 2000 kg to 520 kg due to the 80% decrease of the original contribution from Pd (1600 kg) and Re (250 kg). Further lowering the Pd and Re content to 0.1 wt% cannot significantly increase the cost-effectiveness (**Table 2**, entries 7−9). For example, further lowering the Re content for 80% (from 0.5 to 0.1 wt%) resulted in a 60% decrease in activity (from 0.020

to 0.008 L $h^{-1}$ $g_{cat}^{-1}$). In other words, a great amount of carbon support is needed to balance the saving of Re or Pd in the low metal content range. Again, the *all-in-situ* preparation method allowed the efficient investigation of various metal contents and effectively improved the sustainability of the Re–Pd catalyst system.

**Table 2. Rate Constants of Oxyanion Reductions by Re−Pd/C and Mo−Pd/C with Various Metal Contents.**

| entry | Pd (wt%) | Re or Mo (wt%) | rate constant (L $h^{-1}$ $g_{cat}^{-1}$ )[a] |
|---|---|---|---|
| ***Reduction of 1 mM $ClO_4^-$ with Re−Pd/C*** | | | |
| 1 | 5 | 0 | no reaction |
| 2 | 5 | 5 | 0.037 |
| 3 | 5 | 1 | 0.024 |
| 4 | 1 | 5 | 0.022 |
| 5 | 1 | 1 | 0.021 |
| 6 | 0.5 | 0.5 | 0.020 |
| 7 | 0.5 | 0.1 | 0.008 |
| 8 | 0.1 | 0.5 | 0.005 |
| 9 | 0.1 | 0.1 | <0.001 |
| ***Reduction of 1 mM $ClO_3^-$ with Mo−Pd/C*** | | | |
| 10 | 5 | 0 | 0.854 |
| 11 | 5 | 5 | 20.1 |
| 12 | 1 | 5 | 15.0 |
| 13 | 1 | 1 | 7.8 |
| 14 | 1 | 10 | 15.0 |
| 15 | 0.5 | 5 | 9.6 |

[a]The rate constants were normalized by the catalyst loading of Re−Pd/C (2 g $L^{-1}$) and Mo−Pd/C (0.2 g $L^{-1}$). Reaction conditions: pH =3.0, 1 atm $H_2$, and 20 °C.

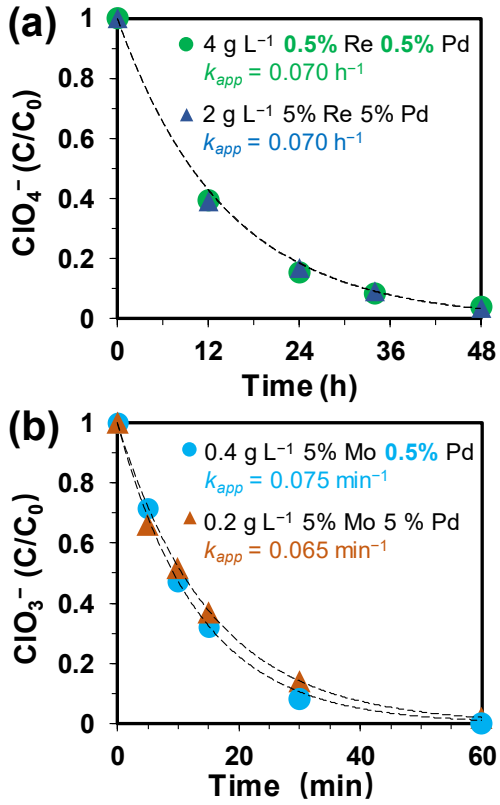


316

317 **Figure 6.** The reduction of (a) 1 mM $ClO_4^-$ by Re–Pd/C with different Re and Pd contents and
318 catalyst loadings and (b) 1 mM $ClO_3^-$ by Mo–Pd/C with different Pd contents and catalyst
319 loadings. Dotted lines indicate the first-order model fit. Reaction conditions: pH =3.0, 1 atm $H_2$,
320 and 20 °C.

321 **Case study 2: Optimization of the Mo–Pd/C catalyst.** We further optimized a Mo–Pd/C
322 catalyst, where both Pd and Mo were 5 wt% for highly active $ClO_3^-$ reduction in the earlier study.[22]
323 Although Pd/C itself can reduce $ClO_3^-$, the immobilization of reduced Mo species on Pd/C
324 substantially enhanced the reaction rate (**Table 2**, entry 11 versus 10). Similar to the redox
325 transformation of Re species, the polymeric $Mo^{VI}O_x$ precursor (from dissolved $Na_2MoO_4$) is
326 reduced by $H_2$+Pd/C into surface-immobilized $Mo^V$, $Mo^{IV}$, $Mo^{III}$, and $Mo^{II}$.[22] $Mo^{IV}$ can abstract
327 one oxygen off the $Mo^{IV}$-bound $ClO_3^-$ and other $x$<3 $ClO_x^-$ products:

328 $$ClO_x^- + Mo^{IV}O_y \rightarrow ClO_{x-1}^- + Mo^{VI}O_{y+1} \qquad (9)$$

329 The $Mo^{IV}$-$Mo^{VI}$ redox cycle is maintained by Pd-catalyzed hydrogenation:

$$Mo^{VI}O_{y+1} + H_2 \rightarrow Mo^{IV}O_y + H_2O \quad (10)$$

Because Mo is an inexpensive metal, our prior interest was to lower the Pd content. With the fixed 5 wt% Mo, we found that the decrease of Pd content from 5 wt% to 0.5 wt% only lowered the $ClO_3^-$ reduction rate for 52% (**Table 2**, entry 15 versus 11). Reducing the Mo content from 5 wt% to 1 wt% also lowered the rate (**Table 2**, entry 13 versus 12). This trend is different from Re–Pd/C (cf. **Table 2**, entry 5 versus 4). However, further adding the Mo content to 10 wt% did not increase the activity (**Table 2**, entry 14 versus 12). A doubled loading (0.4 g $L^{-1}$) of the new 5 wt% Mo – 0.5 wt% Pd/C catalyst achieved the same kinetics as 0.2 g $L^{-1}$ of 5 wt% Mo – 5 wt% Pd/C (**Figure 6b)**, indicating the saving of Pd for 80% without sacrificing the rate of $ClO_3^-$ reduction.

**Implications for reductive catalyst research.** This study shows that Pd-based catalysts of various formulations can be conveniently prepared, evaluated, and optimized for oxyanion reduction applications. As shown by literature[25] and our results using two commercial 1 wt% Pd/C (**Figure S17**), catalysts prepared with different carbon supports and methods can have very different performance. Since the systematic comparison of Pd contents (using the same Pd precursor, support material, and preparation procedures) has not become a common practice in water treatment catalysis research, we attribute this situation to either the multi-step procedures involved in the conventional preparation method or the lack of specialized ovens and furnaces in many water engineering labs.

The *all-in-situ* preparation method only needs 5 min for the adsorption of $Pd^{II}$ precursor and another 5 min for the generation of $Pd^0$ particles. This method only requires 1 atm $H_2$ gas in the headspace, and the water suspension of the catalyst is ready for tests. If only a single-run is needed for the rapid screening of catalyst formulations, this new method minimizes the consumption of materials. For example, to evaluate a 50 mL suspension of 0.1 g $L^{-1}$ Pd/C with

varying Pd contents, only 5 mg of carbon and an even smaller amount of Pd precursor (i.e., 0.5−5 wt%) are needed. In comparison to the oven- and furnace-involved conventional methods, the new method saves time and investment by allowing rapid screening (e.g., **Figure 4** and **Table 2**) and effective optimization (e.g., **Figure 6**) of catalyst formulations. Ultimately, an adequately optimized catalyst will significantly improve the cost-effectiveness and sustainability of catalytic technologies for water treatment.

There are also limitations to this new method. First, it is not suitable for studying catalytic reactions that do not involve $H_2$ (e.g., $Pd^0$-catalyzed oxidation). Second, it cannot be directly applied to prepare granule/pellet catalysts that can be broken into small pieces by stirring. Third, since the method does not involve high temperatures for calcination and reduction, the catalyst may contain residual $Cl^-$ from the $Na_2PdCl_4$ precursor. Literature suggests that a deep removal of $Cl^-$ requires treatment with $H_2$ flow at >200°C.[30] However, high temperatures may cause the sintering of small $Pd^0$ particles into large ones.[26] For synthetic catalysis in organic media or at high temperatures, residual $Cl^-$ can be problematic by producing HCl, contaminating the product, or disrupting the reaction.[46, 47] However, for water treatment catalysis, $Cl^-$ is ubiquitous in water, highly abundant in brine, or produced from the degradation of pollutants (e.g., $ClO_3^-$, $ClO_4^-$, and chlorinated organics). Therefore, the complete removal of $Cl^-$ from the Pd precursor is not necessary for water treatment applications.

## ASSOCIATED CONTENT

### Supporting Information

The Supporting Information is available free of charge at https://pubs.acs.org/doi/10.1021/xxxxx.

Detailed information of catalyst materials; data of CO chemisorption; experimental results for the direct reduction of dissolved and solid $Pd^{II}$ with $H_2$ gas; additional HAADF-STEM and EDS images and XRD spectrum; additional concentration-time profiles for catalytic reactions (PDF).

## AUTHOR INFORMATION


### Corresponding Author

*(J.L.) E-mail: jyliu@engr.ucr.edu; jinyong.liu101@gmail.com.


### Notes

The authors declare no competing financial interest.

## ACKNOWLEDGMENTS


Financial support was provided by the UCR faculty research startup grant for J.L. and the National Science Foundation (CBET-1932942). We thank Dr. Krassimir Bozhilov for performing the STEM characterization at the Central Facility for Advanced Microscopy and Microanalysis (CFAMM) at UC Riverside. We thank Dr. Ich Tran for assisting in the XPS characterization performed at the UC Irvine Materials Research Institute (IMRI) using instrumentation funded in part by the National Science Foundation Major Research Instrumentation Program (CHE-1338173).


## References:


1. Hörold, S.; Vorlop, K.-D.; Tacke, T.; Sell, M., Development of catalysts for a selective nitrate and nitrite removal from drinking water. *Catal. Today* **1993,** *17* (1-2), 21-30.
2. Lecloux, A. J., Chemical, biological and physical constrains in catalytic reduction processes for purification of drinking water. *Catal. Today* **1999,** *53* (1), 23-34.
3. Chaplin, B. P.; Reinhard, M.; Schneider, W. F.; Schüth, C.; Shapley, J. R.; Strathmann, T. J.; Werth, C. J., Critical review of Pd-based catalytic treatment of priority contaminants in water. *Environ. Sci. Technol.* **2012,** *46* (7), 3655-3670.
4. Yin, Y. B.; Guo, S.; Heck, K. N.; Clark, C. A.; Coonrod, C. L.; Wong, M. S., Treating water by degrading oxyanions using metallic nanostructures. *ACS Sustain. Chem. Eng.* **2018,** *6* (9), 11160-11175.
5. Mcnab, W. W.; Ruiz, R.; Reinhard, M., In-situ destruction of chlorinated hydrocarbons in groundwater using catalytic reductive dehalogenation in a reactive well: Testing and operational experiences. *Environ. Sci. Technol.* **2000,** *34* (1), 149-153.
6. Schüth, C.; Kummer, N.-A.; Weidenthaler, C.; Schad, H., Field application of a tailored catalyst for hydrodechlorinating chlorinated hydrocarbon contaminants in groundwater. *Appl. Catal., B* **2004,** *52* (3), 197-203.
7. Davie, M. G.; Cheng, H.; Hopkins, G. D.; LeBron, C. A.; Reinhard, M., Implementing heterogeneous catalytic dechlorination technology for remediating TCE-contaminated groundwater. *Environ. Sci. Technol.* **2008,** *42* (23), 8908-8915.
8. Choe, J. K.; Bergquist, A. M.; Jeong, S.; Guest, J. S.; Werth, C. J.; Strathmann, T. J., Performance and life cycle environmental benefits of recycling spent ion exchange brines by catalytic treatment of nitrate. *Water Res.* **2015,** *80* 267-280.
9. Weinberg, H. S.; Delcomyn, C. A.; Unnam, V., Bromate in chlorinated drinking waters: occurrence and implications for future regulation. *Environ. Sci. Technol.* **2003,** *37* (14), 3104-3110.
10. Butler, R.; Godley, A.; Lytton, L.; Cartmell, E., Bromate environmental contamination: review of impact and possible treatment. *Crit. Rev. Environ. Sci. Technol.* **2005,** *35* (3), 193-217.

11. Stanford, B. D.; Pisarenko, A. N.; Snyder, S. A.; Gordon, G., Perchlorate, bromate, and chlorate in hypochlorite solutions: Guidelines for utilities. *J. Am. Water Works Assoc.* **2011,** *103* (6), 71-83.
12. Bolyard, M.; Fair, P. S.; Hautman, D. P., Occurrence of chlorate in hypochlorite solutions used for drinking water disinfection. *Environ. Sci. Technol.* **1992,** *26* (8), 1663-1665.
13. Alfredo, K.; Stanford, B.; Roberson, J. A.; Eaton, A., Chlorate challenges for water systems. *J. Am. Water Works Assoc.* **2015,** *107* (4), E187-E196.
14. Cho, K.; Qu, Y.; Kwon, D.; Zhang, H.; Cid, C. A.; Aryanfar, A.; Hoffmann, M. R., Effects of anodic potential and chloride ion on overall reactivity in electrochemical reactors designed for solar-powered wastewater treatment. *Environ. Sci. Technol.* **2014,** *48* (4), 2377-2384.
15. Bouchard, D. C.; Williams, M. K.; Surampalli, R. Y., Nitrate contamination of groundwater: sources and potential health effects. *J. Am. Water Works Assoc.* **1992,** *84* (9), 85-90.
16. Bruning-Fann, C. S.; Kaneene, J., The effects of nitrate, nitrite and N-nitroso compounds on human health: A review. *Vet. Hum. Toxicol.* **1993,** *35* (6), 521-538.
17. Gullick, R. W.; Lechevallier, M. W.; Barhorst, T. S., Occurrence of perchlorate in drinking water sources. *J. Am. Water Works Assoc.* **2001,** *93* (1), 66-77.
18. Greer, M. A.; Goodman, G.; Pleus, R. C.; Greer, S. E., Health effects assessment for environmental perchlorate contamination: The dose response for inhibition of thyroidal radioiodine uptake in humans. *Environ. Health Perspect.* **2002,** *110* (9), 927-937.
19. Hurley, K. D.; Shapley, J. R., Efficient heterogeneous catalytic reduction of perchlorate in water. *Environ. Sci. Technol.* **2007,** *41* (6), 2044-2049.
20. Liu, J.; Choe, J. K.; Wang, Y.; Shapley, J. R.; Werth, C. J.; Strathmann, T. J., Bioinspired complex-nanoparticle hybrid catalyst system for aqueous perchlorate reduction: Rhenium speciation and its influence on catalyst activity. *ACS Catal.* **2015,** *5* (2), 511-522.
21. Liu, J.; Choe, J. K.; Sasnow, Z.; Werth, C. J.; Strathmann, T. J., Application of a Re–Pd bimetallic catalyst for treatment of perchlorate in waste ion-exchange regenerant brine. *Water Res.* **2013,** *47* (1), 91-101.
22. Ren, C.; Yang, P.; Gao, J.; Huo, X.; Min, X.; Bi, E. Y.; Liu, Y.; Wang, Y.; Zhu, M.; Liu, J., Catalytic reduction of aqueous chlorate with $MoO_x$ immobilized on Pd/C. *ACS Catal.* **2020,** *10* (15), 8201-8211.
23. Zhou, C.; Wang, Z.; Ontiveros-Valencia, A.; Long, M.; Lai, C.; Zhao, H.; Xia, S.; Rittmann, B. E., Coupling of Pd nanoparticles and denitrifying biofilm promotes $H_2$-based nitrate removal with greater selectivity towards $N_2$. *Appl. Catal., B* **2017,** *206*, 461-470.
24. Choe, J. K.; Mehnert, M. H.; Guest, J. S.; Strathmann, T. J.; Werth, C. J., Comparative assessment of the environmental sustainability of existing and emerging perchlorate treatment technologies for drinking water. *Environ. Sci. Technol.* **2013,** *47* (9), 4644-4652.
25. Mironenko, R. M.; Belskaya, O. B.; Likholobov, V. A., Approaches to the synthesis of Pd/C catalysts with controllable activity and selectivity in hydrogenation reactions. *Catal. Today* **2020,** *357*, 152-165.
26. Xie, Y.; Cao, H.; Li, Y.; Zhang, Y.; Crittenden, J. C., Highly selective PdCu/amorphous silica−alumina (ASA) catalysts for groundwater denitration. *Environ. Sci. Technol.* **2011,** *45* (9), 4066-4072.
27. Shuai, D.; Choe, J. K.; Shapley, J. R.; Werth, C. J., Enhanced activity and selectivity of carbon nanofiber supported Pd catalysts for nitrite reduction. *Environ. Sci. Technol.* **2012,** *46* (5), 2847-2855.

28. Sun, J.; Zhang, J.; Fu, H.; Wan, H.; Wan, Y.; Qu, X.; Xu, Z.; Yin, D.; Zheng, S., Enhanced catalytic hydrogenation reduction of bromate on Pd catalyst supported on $CeO_2$ modified SBA-15 prepared by strong electrostatic adsorption. *Appl. Catal., B* **2018,** *229*, 32-40.
29. Yakukhnov, S. A.; Pentsak, E. O.; Galkin, K. I.; Mironenko, R. M.; Drozdov, V. A.; Likholobov, V. A.; Ananikov, V. P., Rapid "mix-and-stir" preparation of well-defined palladium on carbon catalysts for efficient practical use. *ChemCatChem* **2018,** *10* (8), 1869-1873.
30. Zhao, Y.; Jia, L.; Medrano, J. A.; Ross, J. R.; Lefferts, L., Supported Pd catalysts prepared via colloidal method: the effect of acids. *ACS Catal.* **2013,** *3* (10), 2341-2352.
31. Shao, M.; Yu, T.; Odell, J. H.; Jin, M.; Xia, Y., Structural dependence of oxygen reduction reaction on palladium nanocrystals. *ChemComm* **2011,** *47* (23), 6566-6568.
32. Fagherazzi, G.; Canton, P.; Riello, P.; Pernicone, N.; Pinna, F.; Battagliarin, M., Nanostructural features of Pd/C catalysts investigated by physical methods: A reference for chemisorption analysis. *Langmuir* **2000,** *16* (10), 4539-4546.
33. Vargaftik, M.; Zagorodnikov, V.; Stolyarov, I.; Kochubei, D.; Nekipelov, V. M.; Mastikhin, V.; Chinakov, V.; Zamaraev, K.; Moiseev, I., Formation of palladium hydride complexes upon the reduction of Pd (II) by hydrogen. *Bull. Acad. Sci. USSR, Div. Chem. Sci.* **1985,** *34* (10), 2206-2209.
34. Blokhina, M.; Smirnov, I.; Blokhin, A., Production of fine palladium powders by the hydrogen reduction of palladium hydroxide (II). *Sov. Powder Metall. Met. Ceram.* **1989,** *28* (7), 505-507.
35. Elding, L. I.; Olsson, L. F., Electronic absorption spectra of square-planar chloro-aqua and bromo-aqua complexes of palladium (II) and platinum (II). *J. Phys. Chem.* **1978,** *82* (1), 69-74.
36. Bel'skaya, O.; Gulyaeva, T.; Arbuzov, A.; Duplyakin, V.; Likholobov, V., Interaction between Pt (IV) and Pd (II) chloro complexes in solution and on the $\gamma$-$Al_2O_3$ surface. *Kinet. Catal.* **2010,** *51* (1), 105-112.
37. Zhao, Y.; Liang, W.; Li, Y.; Lefferts, L., Effect of chlorine on performance of Pd catalysts prepared via colloidal immobilization. *Catal. Today* **2017,** *297*, 308-315.
38. Belskaya, O. B.; Mironenko, R. M.; Talsi, V. P.; Rodionov, V. A.; Gulyaeva, T. I.; Sysolyatin, S. V.; Likholobov, V. A., The effect of preparation conditions of Pd/C catalyst on its activity and selectivity in the aqueous-phase hydrogenation of 2,4,6-trinitrobenzoic acid. *Catal. Today* **2018,** *301*, 258-265.
39. Ye, T.; Banek, N. A.; Durkin, D. P.; Hu, M.; Wang, X.; Wagner, M. J.; Shuai, D., Pd nanoparticle catalysts supported on nitrogen-functionalized activated carbon for oxyanion hydrogenation and water purification. *ACS Appl. Nano Mater.* **2018,** *1* (12), 6580-6586.
40. Shuai, D.; McCalman, D. C.; Choe, J. K.; Shapley, J. R.; Schneider, W. F.; Werth, C. J., Structure sensitivity study of waterborne contaminant hydrogenation using shape- and size-controlled Pd nanoparticles. *ACS Catal.* **2013,** *3* (3), 453-463.
41. Chen, X.; Huo, X.; Liu, J.; Wang, Y.; Werth, C. J.; Strathmann, T. J., Exploring beyond palladium: Catalytic reduction of aqueous oxyanion pollutants with alternative platinum group metals and new mechanistic implications. *Chem. Eng. J.* **2017,** *313*, 745-752.
42. Liu, J.; Han, M.; Wu, D.; Chen, X.; Choe, J. K.; Werth, C. J.; Strathmann, T. J., A new bioinspired perchlorate reduction catalyst with significantly enhanced stability via rational tuning of rhenium coordination chemistry and heterogeneous reaction pathway. *Environ. Sci. Technol.* **2016,** *50* (11), 5874-5881.
43. Choe, J. K.; Boyanov, M. I.; Liu, J.; Kemner, K. M.; Werth, C. J.; Strathmann, T. J., X-ray spectroscopic characterization of immobilized rhenium species in hydrated rhenium–palladium

bimetallic catalysts used for perchlorate water treatment. *J. Phys. Chem. C* **2014,** *118* (22), 11666-11676.
44. Hurley, K. D.; Zhang, Y.; Shapley, J. R., Ligand-enhanced reduction of perchlorate in water with heterogeneous Re−Pd/C catalysts. *J. Am. Chem. Soc.* **2009,** *131* (40), 14172-14173.
45. Davie, M. G.; Reinhard, M.; Shapley, J. R., Metal-catalyzed reduction of N-nitrosodimethylamine with hydrogen in water. *Environ. Sci. Technol.* **2006,** *40* (23), 7329-7335.
46. Simone, D. O.; Kennelly, T.; Farrauto, R. J., Reversible poisoning of palladium catalysts for methane oxidation. *Appl. Catal.* **1991,** *70* (1), 87-100.
47. Sepulveda, J.; Figoli, N., Effect of residual chlorine on the activity of $Pd/SiO_2$ catalysts during the selective hydrogenation of styrene. *React. Kinet. Catal. Lett.* **1994,** *53* (1), 155-160.